Chemical Physics Letters 683 (2017) 507–514

Contents lists available at ScienceDirect

Chemical Physics Letters

journal homepage: www.elsevier.com/locate/cplett

Research paper

Excitonic coupling effect on the nonradiative decay rate in molecular aggregates: Formalism and application

Wenqiang Li [a,1], Lili Zhu [a,1], Qiang Shi [b], Jiajun Ren [a], Qian Peng [b,*], Zhigang Shuai [a,*]

[a] Key Laboratory of Organic Optoelectronics and Molecular Engineering, Department of Chemistry, Tsinghua University, Beijing 100084, PR China
[b] Beijing National Laboratory for Molecular Sciences (BNLMS), Institute of Chemistry, Chinese Academy of Sciences, Zhongguancun, Beijing 100190, PR China

ARTICLE INFO

Article history:
Received 12 January 2017
In final form 28 March 2017
Available online 31 March 2017

Keywords:
Organic molecular aggregates
Nonradiative decay rate
Excitonic coupling
Vibronic coupling
Thermal vibration correlation function

ABSTRACT

We present here an analytical thermal vibration correlation function formalism to calculate the nonradiative decay rate constant (k_{nr}) considering excitonic coupling effect (ECE) for molecular aggregates based on split-operator approximation. Combining with first-principles calculations, we found that k_{nr} is enhanced by ECE for both H- and J-aggregates. In addition, ECE is found to be minor for the AIEgens (aggregation-induced emission luminogens).

1. Introduction

Solid-phase photophysical processes determine the optical properties of organic luminescent materials, such as organic nanoparticles [1], thin films [2] and crystals [3]. The photophysical properties of organic molecular aggregates can be different from in solution phase due to a number of intermolecular interactions, such as excitonic coupling and electrostatic interaction, as well as charge transfer. [4] The excitonic coupling effect (ECE) on optical spectra has been widely investigated in organic molecular aggregates [5–13]. It has been long established that H-aggregate exhibits blue-shifted absorption and diminishingly weak (red-shifted) emission intensity, while J-aggregate presents red-shifted absorption and enhanced emission. [13,14] Nevertheless, our understanding of ECE on the nonradiative decay is extremely limited. Early, Freed claimed that the nonradiative transitions between the symmetric and antisymmetric Frenkel-exciton states are strictly forbidden by analyzing the nonadiabatic coupling through the zeroth-order representation [15]. Scharf and Dinur found that the nonradiative decay rate decreases drastically with aggregate size in the strong coupling limit for constant energy gap [16].

Huang and Rhys first proposed the quantitative non-radiative transition rate theory in *F*-centers by considering the strength of the coupling between the electron and the lattice [17]. Then, Lin [18], Jortner and Englman [19,20] extended the theory into the treatment of an isolated polyatomic molecule. In their treatments, the linear displaced oscillator model and the promoting-mode approximation were usually adopted. In recent years, in the context of understanding the aggregation-induced emission phenomena, we developed an analytical nonradiative transition rate theory with Dushinsky rotation effect [21,22] going beyond the promoting-mode approximation by using the thermal vibration correlation function (TVCF) approach [23]. TVCF is an analytical time-integrated rate formalism that can be efficiently solved by fast-Fourier transformation technique. All the vibrational modes and vibronic coupling at the molecular level can be taken into accounts. In this work, we further extended such analytical rate theory to tackle molecular aggregates by considering excitonic coupling effect within the Frenkel exciton model. By dividing the Hamiltonian into intra- and inter-molecular parts, we treat the latter by employing split-operator approximation. Then, it is convenient to construct TVCF and derive an analytical formula to calculate the nonradiative decay rate constant of an aggregate.

We then applied this formalism coupled with the hybrid quantum mechanics and molecular mechanics (QM/MM) calculations to explore the ECE on the nonradiative decay rate constants for a conjugated planar 2,3-dicyanopyrazino phenanthrene (DCPP) [24,25] as well as for four typical AIEgens (aggregation-induced emission luminogens), 2,3-dicyano-5,6-diphenylpyrazine (DCDPP) [26], 1,2-diphenyl-3,4-bis(diphenylmethylene)-1-cyclobutene (CB) [27,28], 1,1,2,3,4,5-hexaphenylsilole (HPS) [29,30], 1,1,3,4-tetraphenyl-2,5-bis(9,9-dimethylfluoren-2-yl)silole (BFTPS) [31,32], see Fig. 1.

* Corresponding authors.
E-mail addresses: qpeng@iccas.ac.cn (Q. Peng), zgshuai@tsinghua.edu.cn (Z. Shuai).
[1] These authors contributed equally.

http://dx.doi.org/10.1016/j.cplett.2017.03.077
0009-2614/

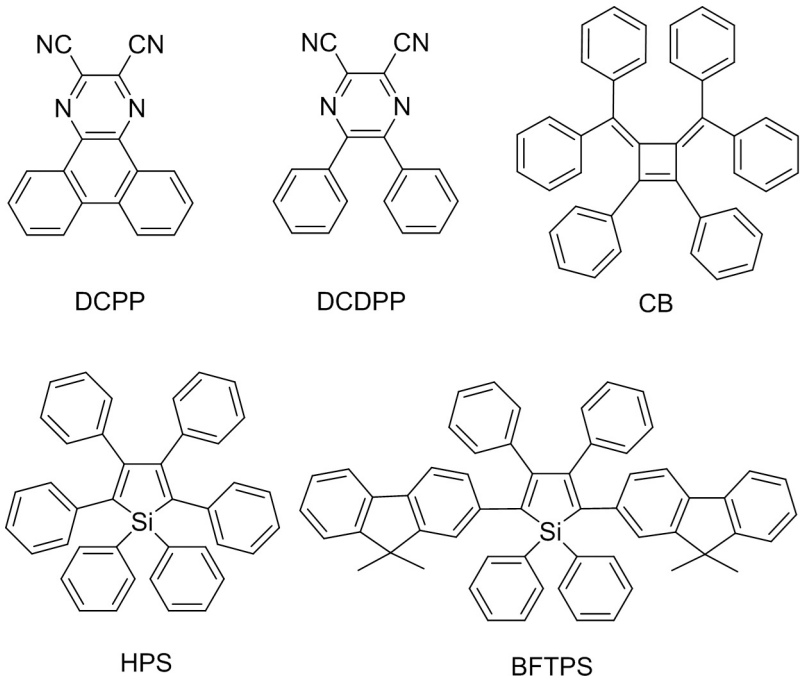

Fig. 1. Molecular structures of the studied molecules.

These can provide a deeper understanding of the effect of intermolecular excited-state interaction on the luminescent property in organic molecular aggregates.

2. Formalism

In this section, we are going to derive an analytical nonradiative decay rate formalism for molecular aggregates in the weak coupling limit. Based on Fermi's Golden Rule (FGR), the nonradiative decay rate constant can be expressed as [21]

$$k_{\mathrm{nr}} = \int_{-\infty}^{\infty} \mathrm{d}t e^{i\Delta E t}\rho(t) \tag{1}$$

$$\rho(t) = \frac{1}{Z_{\mathrm{e}}}\mathrm{Tr}\left[e^{\frac{i\widehat{H}_0 t}{\hbar}}\widehat{H}' e^{\frac{-i\widehat{H}_0 t}{\hbar}}\widehat{H}' e^{-\beta\widehat{H}_{\mathrm{e}}}\right] \tag{2}$$

where $\rho(t)$ is the TVCF of internal conversion. $\widehat{H}_0$ is the zeroth-order Hamiltonian. $\widehat{H}_{\mathrm{e}}$ is the Hamiltonian of the initial state, which is the first excited state in the internal conversion process from S_1 to S_0. $\widehat{H}'$ is the Born-Oppenheimer (non-adiabatic) coupling arising from the nuclear kinetic term. ΔE is the energy difference between the initial and final states. Z_{e} is the partition function of the initial state. $\beta = (k_{\mathrm{B}}T)^{-1}$, where k_{B} is the Boltzmann constant and T the temperature.

Firstly, we take a dimer system to build the basis function, which reads

$$|\psi_1\rangle = |\mathrm{g}(1)\rangle \otimes |\mathrm{g}(2)\rangle, \quad |\psi_2\rangle = |\mathrm{e}(1)\rangle \otimes |\mathrm{g}(2)\rangle, \quad |\psi_3\rangle = |\mathrm{g}(1)\rangle \otimes |\mathrm{e}(2)\rangle, \tag{3}$$

where (1) and (2) are the first and second molecule of the dimer, respectively. Under Condon approximation, these can be recast as

$$|\psi_1\rangle = |\mathrm{g}\rangle|Q_1 \otimes Q_2\rangle, \quad |\psi_2\rangle = |\mathrm{e}_1\rangle|Q_1' \otimes Q_2\rangle, \quad |\psi_3\rangle = |\mathrm{e}_2\rangle|Q_1 \otimes Q_2'\rangle, \tag{4}$$

where

$$|\mathrm{g}\rangle = |\phi_{1\mathrm{g}}\rangle \otimes |\phi_{2\mathrm{g}}\rangle, \quad |\mathrm{e}_1\rangle = |\phi_{1\mathrm{e}}\rangle \otimes |\phi_{2\mathrm{g}}\rangle, \quad |\mathrm{e}_2\rangle = |\phi_{1\mathrm{g}}\rangle \otimes |\phi_{2\mathrm{e}}\rangle, \tag{5}$$

Q (Q') is the harmonic vibrational complete set at the ground (excited) state $\phi_{1\mathrm{g}}$ ($\phi_{1\mathrm{e}}$) and $\phi_{2\mathrm{g}}$ ($\phi_{2\mathrm{e}}$) are the electronic wave functions of molecule **1** and **2** at the ground (excited) state, respectively. Thus, the zeroth-order Hamiltonian for the dimer system can be expanded in the electronic wave function basis as

$$\widehat{H}_0 = \begin{bmatrix} \widehat{H}_{1\mathrm{g}} + \widehat{H}_{2\mathrm{g}} & 0 & 0 \\ 0 & \widehat{H}_{1\mathrm{e}} + \widehat{H}_{2\mathrm{g}} & J \\ 0 & J & \widehat{H}_{1\mathrm{g}} + \widehat{H}_{2\mathrm{e}} \end{bmatrix}, \tag{6}$$

and

$$\widehat{H}' = \sum_k \sum_n^2 [\langle \mathrm{e}_n|\widehat{T}_{nk}|\mathrm{g}\rangle + \langle \mathrm{e}_n|\widehat{P}_{nk}|\mathrm{g}\rangle\widehat{P}_{nk}](|\mathrm{e}_n\rangle\langle \mathrm{g}| + |\mathrm{g}\rangle\langle \mathrm{e}_n|). \tag{7}$$

Here, $\widehat{H}_{ng}$ ($\widehat{H}_{ne}$) is the harmonic Hamiltonian of the nth monomer at the ground (excited) state; J is the excitonic coupling; $\widehat{T}_{nk} = -\frac{\hbar^2}{2}\frac{\partial^2}{\partial^2 q_{nk}}$ and $\widehat{P}_{nk} = -i\hbar\frac{\partial}{\partial q_{nk}}$ where q_{nk} is the normal coordinate of the kth normal mode for the nth monomer. The first term in Eq. (7) is much smaller than the second term in most cases and is often neglected [18]. Thus, Eq. (7) can be rewritten as

$$\widehat{H}' = \sum_k R_{1k}\widehat{P}_{1k}(|\mathrm{e}_1\rangle\langle \mathrm{g}| + |\mathrm{g}\rangle\langle \mathrm{e}_1|) + R_{2k}\widehat{P}_{2k}(|\mathrm{e}_2\rangle\langle \mathrm{g}| + |\mathrm{g}\rangle\langle \mathrm{e}_2|), \tag{8}$$

in which

$$R_{nk} \equiv \langle \phi_{n\mathrm{g}}|\widehat{P}_{nk}|\phi_{n\mathrm{e}}\rangle \tag{9}$$

is the intramolecular nonadiabatic coupling matrix elements (NACMEs). Inserting Eq. (6) into Eq. (2), the TVCF becomes

$$\rho(t)=\frac{1}{Z_e}\sum_k\sum_l\Big[R_{1k}R_{1l}\langle Q_1'\otimes Q_2|\widehat{P}_{1k}e^{-\frac{i\widehat{H}_g t}{\hbar}}\widehat{P}_{1l}\langle e_1|e^{-\frac{i\widehat{H}_e}{\hbar}(-i\hbar\beta-t)}|e_1\rangle|Q_1'\otimes Q_2\rangle$$
$$+R_{1k}R_{2l}\langle Q_1'\otimes Q_2|\widehat{P}_{1k}e^{-\frac{i\widehat{H}_g t}{\hbar}}\widehat{P}_{2l}\langle e_2|e^{-\frac{i\widehat{H}_e}{\hbar}(-i\hbar\beta-t)}|e_1\rangle|Q_1'\otimes Q_2\rangle$$
$$+R_{2k}R_{1l}\langle Q_1\otimes Q_2'|\widehat{P}_{2k}e^{-\frac{i\widehat{H}_g t}{\hbar}}\widehat{P}_{1l}\langle e_1|e^{-\frac{i\widehat{H}_e}{\hbar}(-i\hbar\beta-t)}|e_2\rangle|Q_1\otimes Q_2'\rangle$$
$$+R_{2k}R_{2l}\langle Q_1\otimes Q_2'|\widehat{P}_{2k}e^{-\frac{i\widehat{H}_g t}{\hbar}}\widehat{P}_{2l}\langle e_2|e^{-\frac{i\widehat{H}_e}{\hbar}(-i\hbar\beta-t)}|e_2\rangle|Q_1\otimes Q_2'\rangle\Big] \tag{10}$$

where $\widehat{H}_g=\widehat{H}_{1g}+\widehat{H}_{2g}$, and $\widehat{H}_e$ is

$$\begin{pmatrix}\widehat{H}_{1e}+\widehat{H}_{2g} & J\\ J & \widehat{H}_{1g}+\widehat{H}_{2e}\end{pmatrix}=\underbrace{\begin{pmatrix}\widehat{H}_{1e}+\widehat{H}_{2g} & 0\\ 0 & \widehat{H}_{1g}+\widehat{H}_{2e}\end{pmatrix}}_{\boldsymbol{A}}+\underbrace{\begin{pmatrix}0 & J\\ J & 0\end{pmatrix}}_{\boldsymbol{B}}. \tag{11}$$

To solve Eq. (11), the split-operator approximation is adopted

$$e^{-\frac{it}{\hbar}(\boldsymbol{A}+\boldsymbol{B})}\approx e^{-\frac{it}{2\hbar}\boldsymbol{B}}e^{-\frac{it}{\hbar}\boldsymbol{A}}e^{-\frac{it}{2\hbar}\boldsymbol{B}}, \tag{12}$$

and

$$e^{-\frac{it}{\hbar}\widehat{H}_e}=\begin{pmatrix}e^{-\frac{it}{\hbar}(\widehat{H}_{1e}+\widehat{H}_{2g})}\cos^2\frac{Jt}{2\hbar}+e^{-\frac{it}{\hbar}(\widehat{H}_{1g}+\widehat{H}_{2e})}\sin^2\frac{Jt}{2\hbar} & \left[e^{-\frac{it}{\hbar}(\widehat{H}_{1e}+\widehat{H}_{2g})}+e^{-\frac{it}{\hbar}(\widehat{H}_{1g}+\widehat{H}_{2e})}\right]\sin\frac{Jt}{2\hbar}\cos\frac{Jt}{2\hbar}\\ \left[e^{-\frac{it}{\hbar}(\widehat{H}_{1e}+\widehat{H}_{2g})}+e^{-\frac{it}{\hbar}(\widehat{H}_{1g}+\widehat{H}_{2e})}\right]\sin\frac{Jt}{2\hbar}\cos\frac{Jt}{2\hbar} & e^{-\frac{it}{\hbar}(\widehat{H}_{1e}+\widehat{H}_{2g})}\sin^2\frac{Jt}{2\hbar}+e^{-\frac{it}{\hbar}(\widehat{H}_{1g}+\widehat{H}_{2e})}\cos^2\frac{Jt}{2\hbar}\end{pmatrix} \tag{13}$$

It should be noted that such approximation requires J be small with respect to the intramolecular vibronic coupling. Then, the TVCF turns out to be

$$\rho(t)=\frac{1}{Z_e}\sum_k\sum_l R_{1k}R_{1l}\Big\{\langle Q_1'Q_2|\widehat{P}_{1k}e^{-\frac{i\widehat{H}_g t}{\hbar}}\widehat{P}_{1l}\Big[e^{-\frac{i}{\hbar}(-i\hbar\beta-t)(\widehat{H}_{1e}+\widehat{H}_{2g})}\cos^2\frac{Jt}{2\hbar}+e^{-\frac{i}{\hbar}(-i\hbar\beta-t)(\widehat{H}_{1g}+\widehat{H}_{2e})}\sin^2\frac{Jt}{2\hbar}\Big]|Q_1'Q_2\rangle$$
$$+R_{1k}R_{2l}\langle Q_1'Q_2|\widehat{P}_{1k}e^{-\frac{i\widehat{H}_g t}{\hbar}}\widehat{P}_{2l}\Big[e^{-\frac{i}{\hbar}(-i\hbar\beta-t)(\widehat{H}_{1e}+\widehat{H}_{2g})}+e^{-\frac{i}{\hbar}(-i\hbar\beta-t)(\widehat{H}_{1g}+\widehat{H}_{2e})}\Big]\sin\cos\frac{Jt}{2\hbar}|Q_1'Q_2'\rangle$$
$$+R_{2k}R_{1l}\langle Q_1Q_2'|\widehat{P}_{2k}e^{-\frac{i\widehat{H}_g t}{\hbar}}\widehat{P}_{1l}\Big[e^{-\frac{i}{\hbar}(-i\hbar\beta-t)(\widehat{H}_{1e}+\widehat{H}_{2g})}+e^{-\frac{i}{\hbar}(-i\hbar\beta-t)(\widehat{H}_{1g}+\widehat{H}_{2e})}\Big]\sin\cos\frac{Jt}{2\hbar}|Q_1Q_2'\rangle$$
$$+R_{2k}R_{2l}\langle Q_1Q_2'|\widehat{P}_{2k}e^{-\frac{i\widehat{H}_g t}{\hbar}}\widehat{P}_{2l}\Big[e^{-\frac{i}{\hbar}(-i\hbar\beta-t)(\widehat{H}_{1e}+\widehat{H}_{2g})}\sin^2\frac{Jt}{2\hbar}+e^{-\frac{i}{\hbar}(-i\hbar\beta-t)(\widehat{H}_{1g}+\widehat{H}_{2e})}\cos^2\frac{Jt}{2\hbar}\Big]|Q_1Q_2'\rangle\Big\} \tag{14}$$

Thus, the propagator of an aggregate can be written as the multiplication of monomer. For instance, the first term (denoted as term$_1$ hereafter) in Eq. (14) reads

$$\begin{aligned}\text{term}_1&=R_{1k}R_{1l}\langle Q_1'Q_2|\widehat{P}_{1k}e^{-\frac{i\widehat{H}_g t}{\hbar}}\widehat{P}_{1l}e^{-\frac{i}{\hbar}(-i\hbar\beta-t)(\widehat{H}_{1e}+\widehat{H}_{2g})}|Q_1'Q_2\rangle\\&=R_{1k}R_{1l}\langle Q_1'|\widehat{P}_{1k}e^{-\frac{i\widehat{H}_{1g}t}{\hbar}}\widehat{P}_{1l}e^{-\frac{i\widehat{H}_{1e}}{\hbar}(-i\hbar\beta-t)}|Q_1'\rangle\times\langle Q_2|e^{-\frac{i\widehat{H}_{2g}t}{\hbar}}e^{-\frac{i\widehat{H}_{2g}}{\hbar}(-i\hbar\beta-t)}|Q_2\rangle\end{aligned} \tag{15}$$

Table 1
The abbreviation of the eight terms in Eq. (14).

	Molecule 1	Molecule 2
1	$\delta\delta_k'e^g\delta_l'\delta e^e$	e^ge^g
2	$\delta\delta_k'e^g\delta_l'e^g\delta$	$e^g\delta e^e\delta$
3	$\delta\delta_k'e^g\delta e^e$	$e^g\delta_k'e^g$
4	$\delta\delta_k'e^ge^g\delta$	$e^g\delta_k'\delta e^e\delta$
5	$e^g\delta_k'\delta e^e\delta$	$\delta\delta_k'e^ge^g\delta$
6	$e^g\delta_k'e^g$	$\delta\delta_k'e^g\delta e^e$
7	$e^g\delta e^e\delta$	$\delta\delta_k'e^g\delta_l'e^g\delta$
8	e^ge^g	$\delta\delta_k'e^g\delta_l'\delta e^e$

By inserting the vibrational complete set, the term$_1$ becomes

$$\text{term}_1=\underbrace{\langle Q_1'|X_1\rangle}_{\delta}\underbrace{\langle X_1|\widehat{P}_{1k}|Y_1\rangle}_{\delta_k'}\underbrace{\langle Y_1|e^{-\frac{i\widehat{H}_{1g}t}{\hbar}}|Z_1\rangle}_{e^g}\underbrace{\langle Z_1|\widehat{P}_{1l}|W_1\rangle}_{\delta_l'}\underbrace{\langle W_1|U_1'\rangle}_{\delta}$$
$$\times\underbrace{\langle U_1'|e^{-\frac{i\widehat{H}_{1e}}{\hbar}(-i\hbar\beta-t)}|Q_1'\rangle}_{e^e}\underbrace{\langle Q_2|e^{-\frac{i\widehat{H}_{2g}t}{\hbar}}|X_2\rangle}_{e^g}\underbrace{\langle X_2|e^{-\frac{i\widehat{H}_{2g}}{\hbar}(-i\hbar\beta-t)}|Q_2\rangle}_{e^g}, \tag{16}$$

The other seven terms in Eq. (14) can be handled in the same way and all the relevant propagators are listed in Table 1.

The terms 3, 4, 5 and 6 terms are null because $e^g\delta_k'e^g$ and $\delta\delta_k'e^ge^g\delta$ are zero (a detailed derivation can be found in Appendix A). Thus, Eq. (14) can be recast as

$$\rho(t)=\frac{1}{Z_e}\sum_k\sum_l\Big\{2\Big[\cos^2\frac{J(i\hbar\beta+t)}{2\hbar}\Big](\delta\delta_k'e^g\delta_l'\delta e^e)_1(e^ge^g)_2$$
$$-2\Big[\sin^2\frac{J(i\hbar\beta+t)}{2\hbar}\Big](\delta\delta_k'e^g\delta_l'e^g\delta)_1(e^g\delta e^e\delta)_2\Big\} \tag{17}$$

Herein, $\delta\delta_k'e^g\delta_l'\delta e^e$ is completely the same as the TVCF of a single molecule we developed previously [22]. The solutions of the other terms (e^ge^g, $\delta\delta_k'e^g\delta_l'e^g\delta$, $e^g\delta e^e\delta$) are given in Appendix B and those of the partition function Z_e is presented in Appendix C.

Once we have the TVCF of the dimer in hand, it is straightforward to generalize it to an aggregate with N molecules. The zeroth-order Hamiltonian of the aggregate can be written as

$$\widehat{\boldsymbol{H}}_0 = \begin{pmatrix} \sum_n^N \widehat{H}_{ng} & 0 & 0 & \cdots & 0 \\ 0 & \widehat{H}_{1e} + \sum_{n\neq 1}^N \widehat{H}_{ng} & J_{12} & \cdots & J_{1N} \\ 0 & J_{21} & \ddots & & \vdots \\ \vdots & \vdots & & \ddots & \vdots \\ 0 & J_{N1} & \cdots & \cdots & \widehat{H}_{Ne} + \sum_n^{N-1} \widehat{H}_{ng} \end{pmatrix} \tag{18}$$

The TVCF can be constructed as

$$\begin{aligned} \rho(t) &= \frac{1}{Z_e}\sum_n^N \langle e_n | \langle Q_1 \cdots Q_n' \cdots Q_N | \widehat{H}' e^{-\frac{i\widehat{H}_g t}{\hbar}} \widehat{H}' e^{-\frac{i\widehat{H}_e(-i\hbar\beta - t)}{\hbar}} | Q_1 \cdots Q_n' \cdots Q_N \rangle | e_n \rangle \\ &= \frac{1}{Z_e}\sum_n^N \sum_m^N \sum_{k,l} R_{nk} R_{ml} \langle Q_1 \cdots Q_n' \cdots Q_N | \widehat{P}_{nk} e^{-\frac{i\widehat{H}_g t}{\hbar}} \widehat{P}_{ml} \left\langle e_m \left| e^{-\frac{i\widehat{H}_e(-i\hbar\beta - t)}{\hbar}} \right| e_n \right\rangle | Q_1 \cdots Q_n' \cdots Q_N \rangle \end{aligned} \tag{19}$$

$$\widehat{H}' = \sum_n^N \sum_k R_{nk} \widehat{P}_{nk} (|e_n\rangle\langle g| + |g\rangle\langle e_n|) \tag{20}$$

Matrices A and B in Eq. (12) are defined as

$$\boldsymbol{A} = \begin{pmatrix} \widehat{H}_{1e} + \sum_{n\neq 1}^N \widehat{H}_{ng} & 0 & \cdots & 0 \\ 0 & \ddots & 0 & \vdots \\ \vdots & 0 & \ddots & \vdots \\ 0 & \cdots & \cdots & \widehat{H}_{Ne} + \sum_n^{N-1} \widehat{H}_{ng} \end{pmatrix} \tag{21}$$

$$\boldsymbol{B} = \begin{pmatrix} 0 & J_{12} & \cdots & J_{1N} \\ J_{21} & \ddots & & \vdots \\ \vdots & & \ddots & \vdots \\ J_{N1} & \cdots & \cdots & 0 \end{pmatrix}. \tag{22}$$

And then,

$$e^{-\frac{i(-i\hbar\beta - t)}{2\hbar}\widehat{H}_e} = \begin{pmatrix} \sum_n d_{1n} d_{n1} e^{-\frac{i(-i\hbar\beta - t)}{2\hbar}(\widehat{H}_{1g} + \cdots + \widehat{H}_{ne} + \cdots + \widehat{H}_{Ng})} & \cdots & \sum_n d_{1n} d_{nN} e^{-\frac{i(-i\hbar\beta - t)}{2\hbar}(\widehat{H}_{1g} + \cdots + \widehat{H}_{ne} + \cdots + \widehat{H}_{Ng})} \\ \vdots & & \vdots \\ \sum_n d_{Nn} d_{n1} e^{-\frac{i(-i\hbar\beta - t)}{2\hbar}(\widehat{H}_{1g} + \cdots + \widehat{H}_{ne} + \cdots + \widehat{H}_{Ng})} & \cdots & \sum_n d_{Nn} d_{nN} e^{-\frac{i(-i\hbar\beta - t)}{2\hbar}(\widehat{H}_{1g} + \cdots + \widehat{H}_{ne} + \cdots + \widehat{H}_{Ng})} \end{pmatrix}, \tag{23}$$

where d_{nm} is the element of $e^{-\frac{i(-i\hbar\beta - t)}{2\hbar}\boldsymbol{B}}$ matrix. Thus, Eq. (19) can be expressed as

$$\begin{aligned} C(t) = \frac{1}{Z_e}\sum_n^N \Bigg[& d_{nn}^2 \sum_{kl} R_{nk} R_{nl} (\delta\delta_k' e^g \delta_l' \delta e^e)(e^g e^g)^{N-1} \\ & + \sum_{m\neq n} d_{nm} d_{mn} \sum_{kl} R_{nk} R_{nl} (\delta\delta_k' e^g \delta_l' e^g \delta)(e^g \delta e^e \delta)(e^g e^g)^{N-2} \Bigg], \end{aligned} \tag{24}$$

and it can be solved analytically. Thus, the nonradiative decay rate constant of an aggregate with N molecules can be calculated by using Eq. (1).

3. Computational schemes

All the quantities appeared in the above formalism, such as excited state energy, vibrational modes and vibronic couplings, non-adiabatic coupling, and intermolecular excitonic couplings, are calculated using quantum chemistry packages at the first-principles level. In the electronic structure calculations for molecule, the solid-state environment of the aggregate was mimicked by using QM/MM approach. The computational model was built by cutting a cluster from the X-ray crystal structure, for which the central molecule is treated using QM and the other surrounding molecules using MM. (TD) B3LYP/6-31G(d) [33,34] were adopted to optimize geometry and to calculate the vibrational frequency and transition property for the QM part at the ground and excited states, respectively, using the Turbomole 6.5 program [35,36]. The general Amber force field (GAFF) [37] was employed to deal with the MM part using DL_POLY program [38]. The MM part was kept frozen in the geometry optimization. The QM/MM interface is accomplished by ChemShell 3.5 package [39]. The NACMEs was calculated through evaluating the forces acting on nuclei by transition electric field [21] derived from first-order perturbation [18]. Namely, Eq. (9) can be further expressed as

$$\langle \phi_{ng} | \widehat{P}_{nk} | \phi_{ne} \rangle = -i\hbar \langle \phi_{ng} | \frac{\partial}{\partial Q_{nk}} | \phi_{ne} \rangle \approx -i\hbar \frac{\langle \phi_{ng}^0 | \partial \hat{V}_n / \partial Q_{nk} | \phi_{ne}^0 \rangle}{E_{ne}^0 - E_{ng}^0}. \tag{25}$$

Here

$$\langle \phi_{ng}^0 | \partial \hat{V}_n / \partial Q_{nk} | \phi_{ne}^0 \rangle = -\sum_\sigma \frac{Z_\sigma e^2}{\sqrt{M_\sigma}} \sum_{\tau=x,y,z} E_{ng\leftarrow ne,\sigma\tau} L_{\sigma\tau,nk}, \tag{26}$$

in which

$$E_{ng\leftarrow ne,\sigma\tau} = \int d\mathbf{r} \rho_{fi}^0(\mathbf{r}) e(r_\tau - R_{\sigma\tau}) / |\mathbf{r}_\tau - \mathbf{R}_{\sigma\tau}|^3 \tag{27}$$

is the atomic transition electric field, r and R are the electron and nuclear coordinates, $\rho_{fi}^{0}(\mathbf{r})$ is the electronic transition density. $L_{\sigma\tau,nk} = \partial q_{\sigma\tau}/\partial Q_{nk}$ is a component of the kth eigenvector of the Hessian matrix of nth monomer, Z_σ represents the number of the σth nuclear charge and M_σ is the nuclear mass. $E_{ng\leftarrow ne,\sigma\tau}$ was evaluated using TD/B3LYP/6-31G(d) in the Gaussian 09 package [40]. The excitonic couplings were calculated as Coulomb integral between transition density of different molecules at the level of TD/CAM-B3LYP[41]/6-31G(d) by using our home-built MOMAP program [42] coupled with the NWchem 6.3 program [43]. The nonradiative decay rate constants of the studied compounds were calculated using the formalism derived in this work.

4. Results and discussion

4.1. Effect of excitonic coupling for fully conjugated planar DCPP

DCPP compound has been widely investigated experimentally and theoretically due to its good planar conjugation [24,26,44,45]. Hence, we took DCPP dimer as an example to examine the effect of excitonic coupling on the nonradiative decay rate constant (k_{nr}) as a function of excitonic coupling strength. The calculated k_{nr}s at 298 K are given in Fig. 2(a).

The excitonic coupling effect always enhances k_{nr} regardless of the sign of the excitonic coupling J, whether it's being positive for H-aggregate or negative for J-aggregate [46], because of the squared prefactor in Eq. (17). The k_{nr} obtained at $J = 0$ is completely equal to that of monomer obtained by previous method [22]. And the k_{nr} increases as an approximate quadratic function of J when the J is small because the terms $\cos^2\frac{J(i\hbar\beta+t)}{2\hbar}$ and $\sin^2\frac{J(i\hbar\beta+t)}{2\hbar}$ in Eq. (17) are definitely close to 1 and $\frac{J^2(i\hbar\beta+t)^2}{4\hbar^2}$, as the dash quadratic

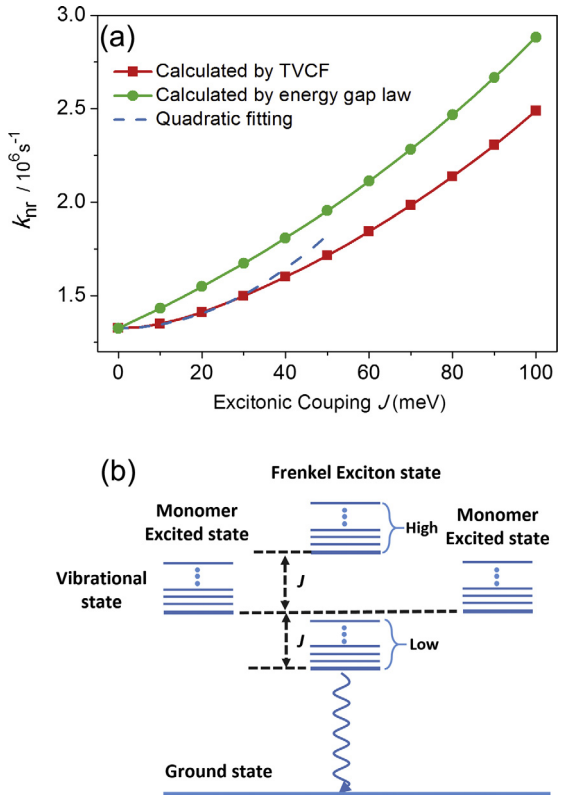

Fig. 2. (a) The nonradiative decay rate constant k_{nr} for DCPP dimer as a function of excitonic coupling strength J at room temperature (298 K), the quadratic fitting function is $k_{nr}^{dimer} = (1 + c \times J^2)k_{nr}^{monomer}$; (b) excited states level splitting for a dimer.

Table 2
Calculated excitonic coupling strength (J), nonradiative decay rate constants with and without J at 298 K and the corresponding ECE for the studied AIEgens.

	J (meV)	$k_{nr}^{without\ J}$ (10^7 s^{-1})	$k_{nr}^{with\ J}$ (10^7 s^{-1})	ECE (%)
DCDPP	0.2–34.2	1.12	1.49	33
CB	−11.6 to 27.1	2.29	2.71	23
HPS	−8.6 to 12.8	2.06	2.31	12
BFTPS	3.1–20.5	8.13	9.85	21

fitting line shown in Fig. 2(a). In general, the excitonic coupling reduces the energy gap of the dimer system [46]. According to the energy gap law for nonradiative decay, k_{nr} increases exponentially with the decrease of the energy gap [20]. The calculated k_{nr}s using the energy gap law from the monomer's are also shown in Fig. 2(a). It is found that the growth rate of k_{nr} calculated by TVCF method is much slower than the one by energy gap law. The deviation arises from the thermal distribution of higher lying Frenkel exciton states (see Fig. 2(b)). In comparison with the monomer, though the k_{nr} of the low-energy FE states is larger, but those for the higher FE states become smaller, leading to an average less than that from energy gap law in Fig. 2(a).

4.2. Effect of excitonic coupling in AIEgens

Aggregation-induced emission (AIE) has been a research hotspot in the field of luminescence materials and photophysics owing to its exotic photophysical property and potential applications [47,48]. This is because conventional luminogens always experience aggregation-caused quenching due to many reasons, including intermolecular charge separation, energy transfer to quenching sites, or Davydov splitting induced symmetry restriction. A lot of works have been carried out to reveal the mechanism of the exotic AIE phenomena [26,28,30,32,49]. It has been found that the decrease of the nonradiative decay rate in aggregate phase is the primary cause of enhanced emission [47,50]. Generally, the solid-phase luminescent property is presumably affected by the intermolecular excitonic coupling, which is neglected in the previous calculations [26,30]. In a recent work [13], it was found that the optical spectra of AIE systems are almost independent on the excitonic coupling. In this work, we chose the same AIEgens (DCDPP, CB, HPS and BFTPS) as in Ref. [13] to examine the effect of excitonic coupling on the nonradiative decay rate constant.

Considering the delocalization feature of Frenkel exciton, we selected a computational molecular cluster consisting of a central monomer and its most adjacent molecules in the densest packing layer in the X-ray crystal structure (9 molecules for DCDPP, HPS and BFTPS, and 8 molecules for CB) to evaluate the excitonic couplings between molecules (detailed data can be found in Ref. [13]). Before selection, the effect of the cluster size on the nonradiative decay rate constant had been tested by taking the DCDPP as an example. The calculated results of the clusters with 4 molecules (2×2 lattice), 9 molecules (3×3 lattice) and 16 molecules (4×4 lattice) are 1.37×10^7 s^{-1}, 1.49×10^7 s^{-1} and 1.49×10^7 s^{-1}, respectively, which indicate the selected cluster has well balanced the accuracy and computational cost.

Table 2 lists the excitonic coupling strengths and the nonradiative decay rate constants with and without considering excitonic coupling at 298 K. The excitonic coupling effect is defined as $ECE = (k_{nr}^{with\ J} - k_{nr}^{without\ J})/k_{nr}^{without\ J}$. It is seen that the excitonic coupling always enhances the nonradiative decay rate by about 12–33% for the AIEgens. It is also seen that the order of magnitudes of the rates remains unchanged after taking excitonic coupling into account, which indicates the excitonic coupling has is a minor effect on the nonradiative decay in AIEgens.

5. Conclusions

We have derived an analytical thermal vibration correlation function formalism to calculate the nonradiative decay rate constant with excitonic coupling effect for molecular aggregates by virtue of split-operator approximation. When coupled with QM/MM calculations, we investigate the excitonic coupling effects for organic molecular aggregates. We found that: (i) the excitonic coupling always increases nonradiative decay rate constants, completely different from the spectral behavior, the latter depending on the sign of the excitonic coupling; (ii) the excitonic coupling has very minor effect on the nonradiative decay rate for AIEgens, which renders supports to previous investigations on the AIE mechanism ignoring the excitonic effect [22,44,45]. These are helpful for molecular designs for solid-phase luminescence materials.

Acknowledgements

The work is supported by the National Natural Science Foundation of China (Grants 91622121, 21473214, and 21290191), the Ministry of Science and Technology of China through the 973 program (Grants 2013CB834703, 2015CB65502 and 2013CB933503), and the Strategic Priority Research Program of the Chinese Academy of Sciences (Grant XDB12020200).

Appendix A

Proof of $e^{g}\delta'_k e^{g}=0$

$$\begin{aligned}
e^{g}\delta'_k e^{g} &= \left\langle Q\left| e^{-\frac{i\widehat{H}_g t}{\hbar}}\widehat{P}_k e^{\frac{\widehat{iH}_g}{\hbar}(-i\hbar\beta-t)}\right| Q\right\rangle \\
&= \left\langle Q\left| e^{-\frac{i\widehat{H}_g t}{\hbar}}\right| X\right\rangle\langle X|\widehat{P}_k|Y\rangle\left\langle Y\left| e^{\frac{\widehat{iH}_g}{\hbar}(-i\hbar\beta-t)}\right| Q\right\rangle \\
&= \iiint dQdXdY\sqrt{\frac{\det[\boldsymbol{a}]}{(2\pi i\hbar)^N}} \\
&\quad\times\exp\left\{\frac{i}{\hbar}[(Q^T\boldsymbol{b}Q+X^T\boldsymbol{b}X)-Q^T\boldsymbol{a}X]\right\} \\
&\quad\times\left[-i\hbar\delta'(x_k-y_k)\prod_{j\neq k}\delta(x_j-y_j)\right]\times\sqrt{\frac{\det[\boldsymbol{a}']}{(2\pi i\hbar)^N}} \\
&\quad\times\exp\left\{\frac{i}{\hbar}[(Y^T\boldsymbol{b}'Y+Q^T\boldsymbol{b}'Q)-Y^T\boldsymbol{a}'Q]\right\} \\
&= dQdX\sqrt{\frac{\det[\boldsymbol{a}\boldsymbol{a}']}{(2\pi i\hbar)^{2N}}}(b'_k x_k-a'_k q_k) \\
&\quad\times\exp\left\{\frac{i}{\hbar}[X^T\frac{(\boldsymbol{b}+\boldsymbol{b}')}{2}X+Q^T\frac{(\boldsymbol{b}'+\boldsymbol{b})}{2}Q-X^T(\boldsymbol{a}'+\boldsymbol{a})Q]\right\} \\
&= \int dL\sqrt{\frac{\det[\boldsymbol{a}\boldsymbol{a}']}{(2\pi i\hbar)^{2N}}}\boldsymbol{H}^T L\exp\left\{\frac{i}{\hbar}[\frac{1}{2}L^T\boldsymbol{K}'L]\right\}=0,
\end{aligned} \tag{A.1}$$

where

$$\boldsymbol{a}=\begin{bmatrix}\frac{\omega_1^g}{\sin(\hbar\omega_1^g t)} & 0 & 0\\ 0 & \ddots & 0\\ 0 & 0 & \frac{\omega_M^g}{\sin(\hbar\omega_M^g t)}\end{bmatrix}, \tag{A.2}$$

$$\boldsymbol{a}'=\begin{bmatrix}\frac{\omega_1^g}{\sin(\hbar\beta\omega_1^g)} & 0 & 0\\ 0 & \ddots & 0\\ 0 & 0 & \frac{\omega_M^g}{\sin(\hbar\beta\omega_M^g)}\end{bmatrix}, \tag{A.3}$$

$$\boldsymbol{b}=\begin{bmatrix}\frac{\omega_1^g}{\tan(\hbar\omega_1^g t)} & 0 & 0\\ 0 & \ddots & 0\\ 0 & 0 & \frac{\omega_M^g}{\tan(\hbar\omega_M^g t)}\end{bmatrix}, \tag{A.4}$$

$$\boldsymbol{b}'=\begin{bmatrix}\frac{\omega_1^g}{\tan(\hbar\beta\omega_1^g)} & 0 & 0\\ 0 & \ddots & 0\\ 0 & 0 & \frac{\omega_M^g}{\tan(\hbar\beta\omega_M^g)}\end{bmatrix}, \tag{A.5}$$

$$\boldsymbol{H}^T=[0\cdots b'_k\cdots 0\cdots -a'_k\cdots 0], \tag{A.6}$$

$$a'_k=\frac{\omega_k^g}{\sin(\hbar\beta\omega_k^g)},\quad b'_k=\frac{\omega_k^g}{\tan(\hbar\beta\omega_k^g)}, \tag{A.7}$$

$$L=X+Q, \tag{A.8}$$

$$\boldsymbol{K}'=\begin{bmatrix}\boldsymbol{b}+\boldsymbol{b}' & -\boldsymbol{a}-\boldsymbol{a}'\\ -\boldsymbol{a}-\boldsymbol{a}' & \boldsymbol{b}+\boldsymbol{b}'\end{bmatrix}. \tag{A.9}$$

Here, X and Y are the harmonic vibrational complete set, ω_k^g is the frequency of normal mode k in the ground state of the monomer and M is the total number of the normal mode.

Using cyclic invariance of the trace

$$\delta\delta'_k e^{g}e^{g}\delta=\delta'_k e^{g}e^{g}=e^{g}\delta'_k e^{g}=0. \tag{A.10}$$

Appendix B

$$\begin{aligned}
\delta\delta'_k e^{g}\delta'_l\delta e^{e} &= \langle Q'|X\rangle\langle X|\widehat{P}_k|Y\rangle\left\langle Y\left| e^{-\frac{iH_g t}{\hbar}}\right| Z\right\rangle\left\langle Z\left|\widehat{P}_l\right| W\right\rangle\langle W|U'\rangle\left\langle U'\left| e^{\frac{iH_g}{\hbar}(-i\hbar\beta-t)}\right| Q'\right\rangle \\
&= \sqrt{\frac{\det[\boldsymbol{a}\boldsymbol{a}']}{\det[\boldsymbol{K}]}}\{\boldsymbol{F}^T\boldsymbol{K}^{-1}\boldsymbol{G}_{kl}\boldsymbol{K}^{-1}\boldsymbol{F}+i\hbar\mathrm{Tr}[\boldsymbol{G}_{kl}\boldsymbol{K}^{-1}]-\boldsymbol{H}_{kl}^T\boldsymbol{K}^{-1}\boldsymbol{F}\} \\
&\quad\times\exp\left\{\frac{i}{\hbar}[-\frac{1}{2}\boldsymbol{F}^T\boldsymbol{K}^{-1}\boldsymbol{F}+\boldsymbol{D}^T\boldsymbol{E}\boldsymbol{D}]\right\}
\end{aligned} \tag{B.1}$$

where

$$\boldsymbol{K}=\begin{bmatrix}\boldsymbol{B} & -\boldsymbol{A}\\ -\boldsymbol{A} & \boldsymbol{B}\end{bmatrix}, \tag{B.2}$$

$$\boldsymbol{F}=\begin{bmatrix}\boldsymbol{D}^T\boldsymbol{E}\boldsymbol{S} & \boldsymbol{D}^T\boldsymbol{E}\boldsymbol{S}\end{bmatrix}. \tag{B.3}$$

$$\boldsymbol{G}_{kl}=\begin{bmatrix}\cdots & \cdots & \cdots & \cdots & \cdots & \cdots\\ \cdots & 0 & \cdots & \cdots & 0 & \cdots\\ \cdots & -b_k\boldsymbol{N}_{l\to k} & \cdots & \cdots & b_k\boldsymbol{M}_{l\to k} & \cdots\\ \cdots & 0 & \cdots & \cdots & 0 & \cdots\\ \cdots & \cdots & \cdots & \cdots & \cdots & \cdots\\ \cdots & 0 & \cdots & \cdots & 0 & \cdots\\ \cdots & a_k\boldsymbol{N}_{l\to k} & \cdots & \cdots & -a_k\boldsymbol{M}_{l\to k} & \cdots\\ \cdots & 0 & \cdots & \cdots & 0 & \cdots\\ \cdots & \cdots & \cdots & \cdots & \cdots & \cdots\end{bmatrix} \tag{B.4}$$

$$\boldsymbol{H}_{kl} = \begin{bmatrix} \vdots \\ 0 \\ b_k(\boldsymbol{D}^{\mathrm{T}}\boldsymbol{E}\boldsymbol{S})_{l\to k} \\ 0 \\ \vdots \\ 0 \\ -a_k(\boldsymbol{D}^{\mathrm{T}}\boldsymbol{E}\boldsymbol{S})_{l\to k} \\ 0 \end{bmatrix} \tag{B.5}$$

Those parameters are defined as

$$\boldsymbol{A} = \boldsymbol{a} + \boldsymbol{N}, \quad \boldsymbol{B} = \boldsymbol{b} + \boldsymbol{M}, \quad \boldsymbol{S}^{\mathrm{T}}\boldsymbol{b}'\boldsymbol{S} = \boldsymbol{M}, \quad \boldsymbol{S}^{\mathrm{T}}\boldsymbol{a}'\boldsymbol{S} = \boldsymbol{N}, \quad \boldsymbol{E} = \boldsymbol{b}' - \boldsymbol{a}'$$

and $\boldsymbol{S}$ is the Duschinsky rotation matrix of the monomer.

$$\begin{aligned} e^{g}e^{g} &= \langle Q|e^{-\beta H_g}|Q\rangle \\ &= \left[\prod_j 2\sinh(\hbar\beta\omega_j^g/2)\right]^{-1} \end{aligned} \tag{B.6}$$

is the partition function of a monomer on the ground state.

$$\begin{aligned} &\delta\delta'_k e^{g}\delta'_l e^{g}\delta \\ &= \langle Q'|X\rangle\langle X|\widehat{P}_k|Y\rangle\left\langle Y\left|e^{-\frac{iH_g t}{\hbar}}\right|Z\right\rangle\langle Z|\widehat{P}_l|W\rangle\left\langle W\left|e^{-\frac{iH_g}{\hbar}(-i\hbar\beta-t)}\right|U\right\rangle\langle U|Q'\rangle \\ &= \sqrt{\frac{\det[\boldsymbol{a}\boldsymbol{a}']}{\det[\boldsymbol{K}']}}\frac{i\hbar}{\det[\boldsymbol{S}]}\mathrm{Tr}[\boldsymbol{G}'_{kl}\boldsymbol{K}'^{-1}] \end{aligned} \tag{B.7}$$

where

$$\boldsymbol{G}'_{kl} = \begin{bmatrix} \cdots & \cdots & \cdots & \cdots & \cdots & \cdots \\ \cdots & 0 & \cdots & \cdots & 0 & \cdots \\ \cdots & -a'_l b_k & \cdots & \cdots & b'_l a_k & \cdots \\ \cdots & 0 & \cdots & \cdots & 0 & \cdots \\ \cdots & \cdots & \cdots & \cdots & \cdots & \cdots \\ \cdots & 0 & \cdots & \cdots & 0 & \cdots \\ \cdots & a'_l a_k & \cdots & \cdots & -b'_l a_k & \cdots \\ \cdots & 0 & \cdots & \cdots & 0 & \cdots \\ \cdots & \cdots & \cdots & \cdots & \cdots & \cdots \end{bmatrix} \tag{B.8}$$

$$\begin{aligned} e^{g}\delta e^{e}\delta &= \left\langle Q\left|e^{-\frac{i\hbar_g t}{\hbar}}\right|X\right\rangle\langle X|Y'\rangle\left\langle Y'\left|e^{-\frac{i\hbar_e}{\hbar}(-i\hbar\beta-t)}\right|Z'\right\rangle\langle Z'|Q\rangle \\ &= \sqrt{\frac{\det[\boldsymbol{a}\boldsymbol{a}']}{\det[\boldsymbol{K}]}}\exp\left\{\frac{i}{\hbar}\left[-\frac{1}{2}\boldsymbol{F}^T\boldsymbol{K}^{-1}\boldsymbol{F} + \boldsymbol{D}^T\boldsymbol{E}\boldsymbol{D}\right]\right\} \end{aligned} \tag{B.9}$$

Appendix C

As the partition function in dimer case, $Z_e = \mathrm{Tr}[e^{-\beta H_e}]$, we also employ the split operator method to partition the excited Hamiltonian into the vibrational part and the exciton coupling part

$$e^{-\beta\widehat{H}_e} = \begin{bmatrix} \cosh\frac{\beta J}{2} & -\sinh\frac{\beta J}{2} \\ -\sinh\frac{\beta J}{2} & \cosh\frac{\beta J}{2} \end{bmatrix}\begin{bmatrix} e^{-\beta(\widehat{H}_{1e}+\widehat{H}_{2g})} & 0 \\ 0 & e^{-\beta(\widehat{H}_{1g}+\widehat{H}_{2e})} \end{bmatrix}\begin{bmatrix} \cosh\frac{\beta J}{2} & -\sinh\frac{\beta J}{2} \\ -\sinh\frac{\beta J}{2} & \cosh\frac{\beta J}{2} \end{bmatrix}. \tag{C.1}$$

Using cyclic invariance of the trace, and also the identity property of both of the monomer, we can obtain

$$\begin{aligned} Z_e &= \left(\cosh^2\frac{\beta J}{2} + \sinh^2\frac{\beta J}{2}\right)\langle Q'_1 Q_2|e^{-\beta(\widehat{H}_{1e}+\widehat{H}_{2g})}|Q'_1 Q_2\rangle \\ &= 2\left(\cosh^2\frac{\beta J}{2} + \sinh^2\frac{\beta J}{2}\right)\prod_k \frac{1}{2\sinh\frac{\beta\hbar\omega_k^e}{2}}\prod_k \frac{1}{2\sinh\frac{\beta\hbar\omega_k^g}{2}} \end{aligned} \tag{C.2}$$

Appendix D. Supplementary material

Supplementary data associated with this article can be found, in the online version, at http://dx.doi.org/10.1016/j.cplett.2017.03.077.

References

[1] D. Xiao, L. Xi, W. Yang, H. Fu, Z. Shuai, Y. Fang, J. Yao, Size-tunable emission from 1,3-diphenyl-5-(2-anthryl)-2-pyrazoline nanoparticles, J. Am. Chem. Soc. 125 (2003) 6740.

[2] M. Losurdo, M.M. Giangregorio, P. Capezzuto, A. Cardone, C. Martinelli, G.M. Farinola, F. Babudri, F. Naso, M. Büchel, G. Bruno, Blue-gap poly(p-phenylene vinylene)s with fluorinated double bonds: interplay between supramolecular organization and optical properties in thin films, Adv. Mater. 21 (2009) 1115.

[3] S. Varghese, S.-J. Yoon, E.M. Calzado, S. Casado, P.G. Boj, M.A. Díaz-García, R. Resel, R. Fischer, B. Milián-Medina, R. Wannemacher, S.Y. Park, J. Gierschner, Stimulated resonance Raman scattering and laser oscillation in highly emissive distyrylbenzene-based molecular crystals, Adv. Mater. 24 (2012) 6473.

[4] B. Valeur, M.N. Berberan-Santos, Molecular Fluorescence, Wiley-VCH Verlag GmbH & Co, KGaA, 2012.

[5] F.C. Spano, The spectral signatures of Frenkel polarons in H- and J-aggregates, Acc. Chem. Res. 43 (2010) 429.

[6] J. Gierschner, M. Ehni, H.-J. Egelhaaf, B. Milián Medina, D. Beljonne, H. Benmansour, G.C. Bazan, Solid-state optical properties of linear polyconjugated molecules: π-stack contra herringbone, J. Chem. Phys. 123 (2005) 144914.

[7] Z. Zhao, F.C. Spano, Multiple mode exciton-phonon coupling: applications to photoluminescence in oligothiophene thin films, J. Phys. Chem. C 111 (2007) 6113.

[8] Z. Zhao, F.C. Spano, Vibronic fine structure in the absorption spectrum of oligothiophene thin films, J. Chem. Phys. 122 (2005) 114701.

[9] J. Seibt, V. Engel, Absorption and emission spectroscopy of molecular trimers: cyclic versus linear geometries, Chem. Phys. 347 (2008) 120.

[10] H. Liu, L. Zhu, S. Bai, Q. Shi, Reduced quantum dynamics with arbitrary bath spectral densities: hierarchical equations of motion based on several different bath decomposition schemes, J. Chem. Phys. 140 (2014) 134106.

[11] F. Gao, W.Z. Liang, Y. Zhao, Vibrationally resolved absorption and emission spectra of rubrene multichromophores: temperature and aggregation effects, J. Phys. Chem. A 113 (2009) 12847.

[12] J. Seibt, P. Marquetand, V. Engel, Z. Chen, V. Dehm, F. Würthner, On the geometry dependence of molecular dimer spectra with an application to aggregates of perylene bisimide, Chem. Phys. 328 (2006) 354.

[13] W. Li, Q. Peng, Y. Xie, T. Zhang, Z. Shuai, Effect of intermolecular excited-state interaction on vibrationally resolved optical spectra in organic molecular aggregates, Acta Chim. Sinica 74 (2016) 902.

[14] F.C. Spano, Excitons in conjugated oligomer aggregates, films, and crystals, Annu. Rev. Phys. Chem. 57 (2006) 217.

[15] K.F. Freed, Theory of photophysical properties of symmetric chlorophyll hydrated dimers, J. Am. Chem. Soc. 102 (1980) 3130.

[16] B. Scharf, U. Dinur, Striking dependence of the rate of electronic radiationless transitions on the size of the molecular system, Chem. Phys. Lett. 105 (1984) 78.

[17] K. Huang, A. Rhys, Theory of light absorption and non-radiative transitions in F-centers, Proc. Roy. Soc. Lond. 204 (1950) 406.

[18] S.H. Lin, Rate of interconversion of electronic and vibrational energy, J. Chem. Phys. 44 (1966) 3759.

[19] M. Bixon, J. Jortner, Intramolecular radiationless transitions, J. Chem. Phys. 48 (1968) 715.

[20] R. Englman, J. Jortner, The energy gap law for radiationless transitions in large molecules, Mol. Phys. 18 (1970) 145.

[21] Q. Peng, Y. Yi, Z. Shuai, J. Shao, Excited state radiationless decay process with Duschinsky rotation effect: formalism and implementation, J. Chem. Phys. 126 (2007) 114302.

[22] Z. Shuai, Q. Peng, Excited states structure and processes: understanding organic light-emitting diodes at the molecular level, Phys. Rep. 537 (2014) 123.

[23] R. Ianconescu, E. Pollak, Photoinduced cooling of polyatomic molecules in an electronically excited state in the presence of Dushinskii rotations, J. Phys. Chem. A 108 (2004) 7778.

[24] A. Qin, J.W.Y. Lam, F. Mahtab, C.K.W. Jim, L. Tang, J. Sun, H.H.Y. Sung, I.D. Williams, B.Z. Tang, Pyrazine luminogens with "free" and "locked" phenyl rings: understanding of restriction of intramolecular rotation as a cause for aggregation-induced emission, Appl. Phys. Lett. 94 (2009) 253308.

[25] Q. Wu, T. Zhang, Q. Peng, D. Wang, Z. Shuai, Aggregation induced blue-shifted emission – the molecular picture from a QM/MM study, Phys. Chem. Chem. Phys. 16 (2014) 5545.

[26] Q. Wu, C. Deng, Q. Peng, Y. Niu, Z. Shuai, Quantum chemical insights into the aggregation induced emission phenomena: a QM/MM study for pyrazine derivatives, J. Comput. Chem. 33 (2012) 1862.

[27] Y. Dong, J.W.Y. Lam, A. Qin, J. Sun, J. Liu, Z. Li, J. Sun, H.H.Y. Sung, I.D. Williams, H.S. Kwok, B.Z. Tang, Aggregation-induced and crystallization-enhanced emissions of 1,2-diphenyl-3,4-bis(diphenylmethylene)-1-cyclobutene, Chem. Commun. 31 (2007) 3255.

[28] T. Zhang, Q. Peng, C. Quan, H. Nie, Y. Niu, Y. Xie, Z. Zhao, B.Z. Tang, Z. Shuai, Using the isotope effect to probe an aggregation induced emission mechanism: theoretical prediction and experimental validation, Chem. Sci. 7 (2016) 5573.
[29] J. Chen, C.C.W. Law, J.W.Y. Lam, Y. Dong, S.M.F. Lo, I.D. Williams, D. Zhu, B.Z. Tang, Synthesis, light emission, nanoaggregation, and restricted intramolecular rotation of 1,1-substituted 2,3,4,5-tetraphenylsiloles, Chem. Mater. 15 (2003) 1535.
[30] T. Zhang, Y. Jiang, Y. Niu, D. Wang, Q. Peng, Z. Shuai, Aggregation effects on the optical emission of 1,1,2,3,4,5-hexaphenylsilole (HPS): a QM/MM study, J. Phys. Chem. A 118 (2014) 9094.
[31] X. Zhan, A. Haldi, C. Risko, C.K. Chan, W. Zhao, T.V. Timofeeva, A. Korlyukov, M. Y. Antipin, S. Montgomery, E. Thompson, Z. An, B. Domercq, S. Barlow, A. Kahn, B. Kippelen, J.-L. Bredas, S.R. Marder, Fluorenyl-substituted silole molecules: geometric, electronic, optical, and device properties, J. Mater. Chem. 18 (2008) 3157.
[32] Y. Xie, T. Zhang, Z. Li, Q. Peng, Y. Yi, Z. Shuai, Influences of conjugation extent on the aggregation-induced emission quantum efficiency in silole derivatives: a computational study, Chem. – Asian J. 10 (2015) 2154.
[33] A.D. Becke, Density-functional thermochemistry. III. The role of exact exchange, J. Chem. Phys. 98 (1993) 5648.
[34] C. Lee, W. Yang, R.G. Parr, Development of the Colle-Salvetti correlation-energy formula into a functional of the electron density, Phys. Rev. B 37 (1988) 785.
[35] F.C. Spano, L. Silvestri, Multiple mode exciton-vibrational coupling in H-aggregates: synergistic enhancement of the quantum yield, J. Chem. Phys. 132 (2010) 094704.
[36] R. Ahlrichs, M. Bär, M. Häser, H. Horn, C. Kölmel, Electronic structure calculations on workstation computers: the program system turbomole, Chem. Phys. Lett. 162 (1989) 165.
[37] J. Wang, R.M. Wolf, J.W. Caldwell, P.A. Kollman, D.A. Case, Development and testing of a general amber force field, J. Comput. Chem. 25 (2004) 1157.
[38] W. Smith, T.R. Forester, DL_POLY_2.0: a general-purpose parallel molecular dynamics simulation package, J. Mol. Graph. 14 (1996) 136.
[39] P. Sherwood, A.H. de Vries, M.F. Guest, G. Schreckenbach, C.R.A. Catlow, S.A. French, A.A. Sokol, S.T. Bromley, W. Thiel, A.J. Turner, S. Billeter, F. Terstegen, S. Thiel, J. Kendrick, S.C. Rogers, J. Casci, M. Watson, F. King, E. Karlsen, M. Sjøvoll, A. Fahmi, A. Schäfer, C. Lennartz, QUASI: a general purpose implementation of the QM/MM approach and its application to problems in catalysis, J. Mol. Struct. THEOCHEM 632 (2003) 1.
[40] M.J. Frisch, G.W. Trucks, H.B. Schlegel, G.E. Scuseria, M.A. Robb, J.R. Cheeseman, G. Scalmani, V. Barone, B. Mennucci, G.A. Petersson, et al., Gaussian09, revision D.01, Gaussian Inc., Wallingford, CT, 2010.
[41] T. Yanai, D.P. Tew, N.C. Handy, A new hybrid exchange–correlation functional using the Coulomb-attenuating method (CAM-B3LYP), Chem. Phys. Lett. 393 (2004) 51.
[42] Z. Shuai, Q. Peng, Y. Niu, H. Geng, MOMAP. MOMAP, A Free and Open-Source Molecular Materials Property Prediction Package, Beijing, China, Available online: <http://www.shuaigroup.net>, 2016.
[43] M. Valiev, E.J. Bylaska, N. Govind, K. Kowalski, T.P. Straatsma, H.J.J. Van Dam, D. Wang, J. Nieplocha, E. Apra, T.L. Windus, W.A. de Jong, NWChem: a comprehensive and scalable open-source solution for large scale molecular simulations, Comput. Phys. Commun. 181 (2010) 1477.
[44] Z. Shuai, Q. Peng, Organic light-emitting diodes: theoretical understanding of highly efficient materials and development of computational methodology, Nat. Sci. Rev. (2017), http://dx.doi.org/10.1093/nsr/nww024.
[45] T. Zhang, H. Ma, Y. Niu, W. Li, D. Wang, Q. Peng, Z. Shuai, W. Liang, Spectroscopic signature of the aggregation-induced emission phenomena caused by restricted nonradiative decay: a theoretical proposal, J. Phys. Chem. C 119 (2015) 5040.
[46] M. Kasha, H. Rawls, M.A. El-Bayoumi, The exciton model in molecular spectroscopy, Pure Appl. Chem. 11 (1965) 371.
[47] J. Mei, N.L.C. Leung, R.T.K. Kwok, J.W.Y. Lam, B.Z. Tang, Aggregation-induced emission: together we shine, united we soar!, Chem Rev. 115 (2015) 11718.
[48] X.Z. Lim, The nanoscale rainbow, Nature 531 (2016) 26.
[49] X.-L. Peng, S. Ruiz-Barragan, Z.-S. Li, Q.-S. Li, L. Blancafort, Restricted access to a conical intersection to explain aggregation induced emission in dimethyl tetraphenylsilole, J. Mater. Chem. C 4 (2016) 2802.
[50] H. Qian, M.E. Cousins, E.H. Horak, A. Wakefield, M.D. Liptak, I. Aprahamian, Suppression of Kasha's rule as a mechanism for fluorescent molecular rotors and aggregation-induced emission, Nat. Chem. 9 (2016) 83.